Dendrites are more spiny on mature hippocampal neurons when synapses are inactivated

Sergei A. Kirov and Kristen M. Harris

Division of Neuroscience in the Department of Neurology, Children's Hospital and Harvard Medical School, Enders 260, 300 Longwood Ave., Boston, Massachusetts 02115, USA

Correspondence should be addressed to K.M.H. (harrisk@hub.tch.harvard.edu)

Dendrites of CA1 pyramidal neurons in mature rat hippocampal slices were exposed to different levels of synaptic activation. In some slices, synaptic transmission was blocked with glutamate receptor antagonists, sodium and calcium channel blockers and/or a nominally calcium-free medium with high magnesium. In other slices, synapses were activated with low-frequency control stimulation or repeated tetanic stimulation. In slices with blocked synaptic transmission, dendrites were spinier than in either of the activated states. Thus, mature neurons can increase their numbers of spines, possibly compensating for lost synaptic activity.

A longstanding goal in neuroscience has been to understand mechanisms of synaptogenesis. In the central nervous system, this question extends to dendritic spines because the vast majority of excitatory synapses occur on these tiny protrusions from dendrites[1,2]. Several studies explored dendritic spine formation on developing neurons[3,4]. Spine number can either increase or decrease depending on the degree of synapse activation in dissociated neuronal cultures[5–8], in organotypic slices[9–13] and *in vivo*[14–16]. Immature neurons also increase synaptic strength in compensation for lost synaptic activity[17]. It is not known if this increase in synaptic strength is coupled to the formation of new synapses, nor if spines emerge in direct response to synapse activation. Alternatively, spines and synapses may form independently of activation and then be preserved or eliminated by specific patterns of synaptic activity.

Spine number also changes on mature neurons. For example, the number of hippocampal spines in the adult female rat is modulated over a couple of days with changes in hormonal status[18,19]. More spines occur in the cortex after exposure to an enriched environment[20,21], and in the hippocampus after spatial learning[22] in adult rats. Neurons do not obtain an adult complement of dendritic spines and synapses in dissociated cell cultures[23] or in organotypic slices[24,25]; hence, little is known about the role of activation in synaptogenesis and spine formation on mature neurons[26]. To address this question, dendrite spininess was assessed in hippocampal slices from mature rats in which synaptic activity was pharmacologically blocked and in those with low or high levels of synaptic activation.

Results

Small clusters of pyramidal neurons were labeled at the beginning of each experiment by inserting DiI-coated microelectrodes into the CA1 pyramidal cell layer of hippocampal slices at 3 locations about 200 μm apart for approximately 2 minutes[27] (**Fig. 1a**). In the first set of experiments, four different slice conditions were prepared (**Fig. 1b**). One of the four slices in each experiment was maintained in normal control media (see Methods) and received high synaptic activation via sequential tetani (100 Hz for 1 second at half-maximal stimulation) between 2 pathways at 10-minute intervals for 3–4 hours (**Fig. 1b,** Tetanus). These tetanized slices had potentiated synaptic responses relative to the pretetanus baseline recordings. Control slices, also maintained in normal control media, received low-frequency stimulation (once per 30 seconds) and were tested with increasing stimulus intensities to generate an input–output curve (**Fig. 1b,** Control). Tetanus and control slices had equal maximal fEPSP slopes and stable baseline responses. Blocked slices were maintained in a nominally calcium-free media with 8 mM Mg^{2+} plus the activity antagonists TTX, nimodipine, CNQX, APV and MCPG and had no evoked responses (**Fig. 1b,** Block). Other slices were maintained in nominally calcium-free media, and generated a fiber volley but no synaptic response upon extracellular stimulation (**Fig 1b,** 0 Ca^{2+}/8 Mg^{2+}).

Slices were fixed in mixed aldehydes using a microwave-enhanced procedure[28]. Well-isolated secondary branches of the apical dendrites were located about 100–300 μm from stratum pyramidal in the middle of stratum radiatum of hippocampal area CA1 (**Fig. 1c**). Each branch was photographed with confocal microscopy at its tip and along the middle of its length (**Fig. 1d**).

Two strategies were used to assess the spininess of dendrites in each condition (**Fig. 2**). The first strategy was to obtain relative spine densities by counting the visible dendritic spines, measuring the length of the dendritic segment and computing the number of spines per unit length of dendrite (**Fig. 2**, left column). All protrusions from the dendrites were treated as 'spines', though with confocal microscopy it was not possible to know if they had synapses, or if some of them were filopodia[4,5]. In the second strategy, a rank score was assigned by comparing dendrites in all four conditions from a single experiment to a 'proband' dendrite with approximately average spininess for that experiment. All other dendrites in the same experiment were scored relative to the proband dendrite as less (score 1), equally (score 2) or more spiny

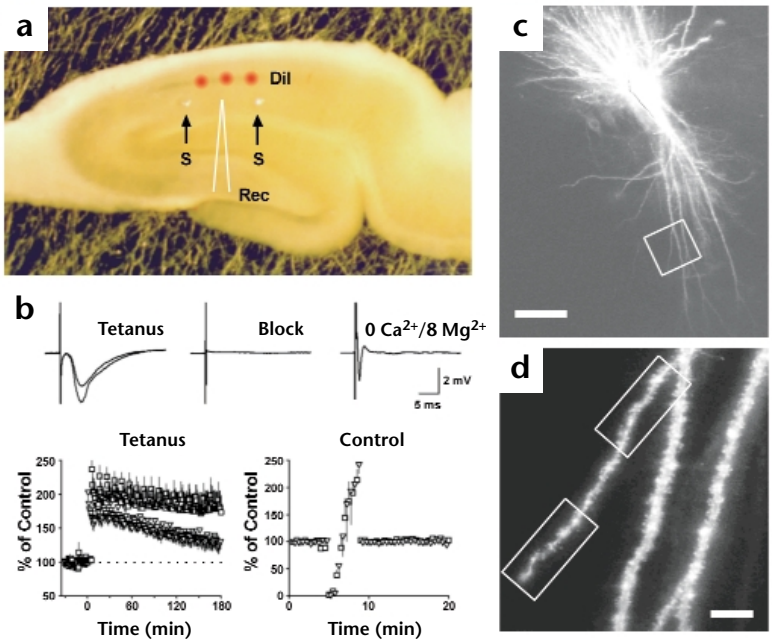

Fig. 1. Imaging and electrophysiological recording in hippocampal slice preparations. (**a**) Position of the stimulating (S) and recording (Rec) electrodes and sites of DiI application into the CA1 pyramidal cell layer (red spots). (**b**) Summary of physiological responses. Top three panels are fEPSPs before (small potential) and after (large potential) tetanic stimulation, in the block condition, and with high stimulus intensity in the 0 Ca^{2+}/8 Mg^{2+} condition. The tetanus graph illustrates the percent change in the mean fEPSP slope during repeated tetanic stimulation starting after time zero (mean ± s.e.; n = 5 slices from five animals; squares, orthodromic stimulation from S electrode on the CA3 side; triangles, antidromic stimulation from the S electrode on the subicular side). Control graph shows the input–output function (mean ± s.e.) for both stimulus pathways (n = 6 slices from six animals). (**c**) Small cluster of pyramidal neurons labeled with DiI in a control slice. Scale bar, 100 μm. (**d**) An extended-focus, higher magnification image of the boxed region in (**c**), made by combining a stack of 28 optical sections spanning 14 μm in the z dimension. Scale bar, 10 μm.

(score 3; **Fig. 2**, right column). All photography and analyses were done blind with regard to experimental conditions.

In the first set of experiments, a total of 870 dendritic segments from 6 animals (4 slices per animal) were analyzed with both methods. In Figs. 3a and 4a, respectively, the tips and middles of the dendrites are arranged from low to high spine density, and matched for percentile rank in spine density across each condition. These figures show pictorially that dendrites are spinier in the two conditions with blocked synaptic activity than in the control or tetanus conditions. Quantitatively, the dendritic tips were spinier in the block and 0 Ca^{2+}/8 Mg^{2+} conditions than in the control or tetanus conditions ($F_{3,434} = 16.57$, $p < 0.001$; **Fig.3b**), with the spine densities increasing 33.8 ± 4.9% for the block ($p < 0.001$) and 23.0 ± 5.7% for the 0 Ca^{2+}/8 Mg^{2+} ($p < 0.001$) conditions relative to the control condition. Dendrite middles were also more spiny in the block and 0 Ca^{2+}/8 Mg^{2+} conditions ($F_{3,434} = 26.63$, $p < 0.001$; **Fig. 4b**), increasing 22.9 ± 4.5% for the block ($p < 0.001$) and 21.1 ± 5.2% for the 0 Ca^{2+}/8 Mg^{2+} ($p < 0.001$) conditions relative to the control condition. Dendritic tips (**Fig. 3c**) and middles (**Fig. 4c**) from slices maintained in the block or 0 Ca^{2+}/8 Mg^{2+} conditions also had higher spine rank scores than dendrites from slices maintained in control or tetanus conditions (both χ^2 and ANOVA on ranks; $p < 0.001$).

There were no significant differences in spine densities or spine rank scores between the control and tetanus conditions, nor between the block and 0 Ca^{2+}/8 Mg^{2+} conditions.

The absolute spine density measured from confocal microscopy was less than half the value obtained from serial EM analyses in slices[26,29]. This difference can be attributed to two factors[30,31]. Only spines emerging from the lateral edges of the dendrites were readily distinguished with confocal microscopy; spines emerging from the back and front were hidden. Second, fluorescence from closely spaced spines made them difficult to resolve, especially when spine density was high, as was true for the mature dendrites. Although confocal microscopy revealed lower absolute values for the spine densities, the relative differences in densities and scores were valid and proved useful in analyzing large numbers of dendrites.

The purpose of a second set of experiments was to determine if

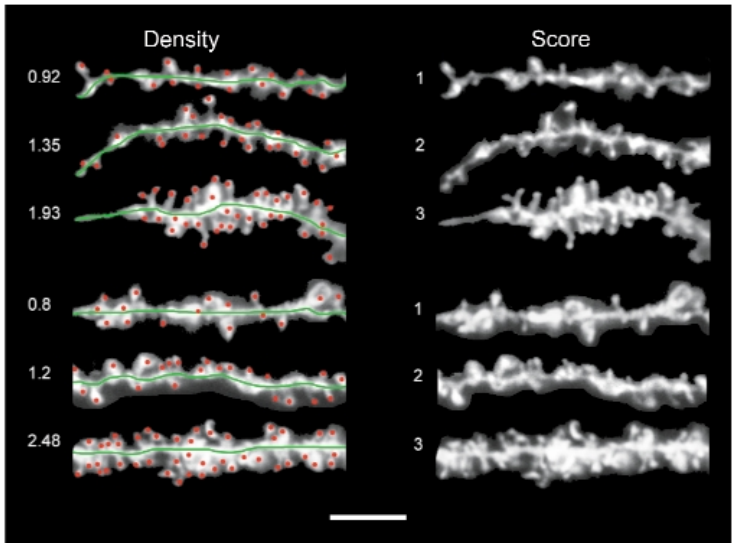

Fig. 2. Two strategies for assessing dendrite spininess. The left column (Density) illustrates the spine density method. All spine-like protrusions (red dots) on dendritic tips (top three rows) and middles (bottom three rows) were counted, and the lengths of dendritic segments were measured (green lines). Spine densities are indicated to the left of each dendrite. The right column (Score) of dendrites demonstrates the method for rank scoring the dendrite spininess. The same dendrites are illustrated for each method. Scale bar, 5 μm.

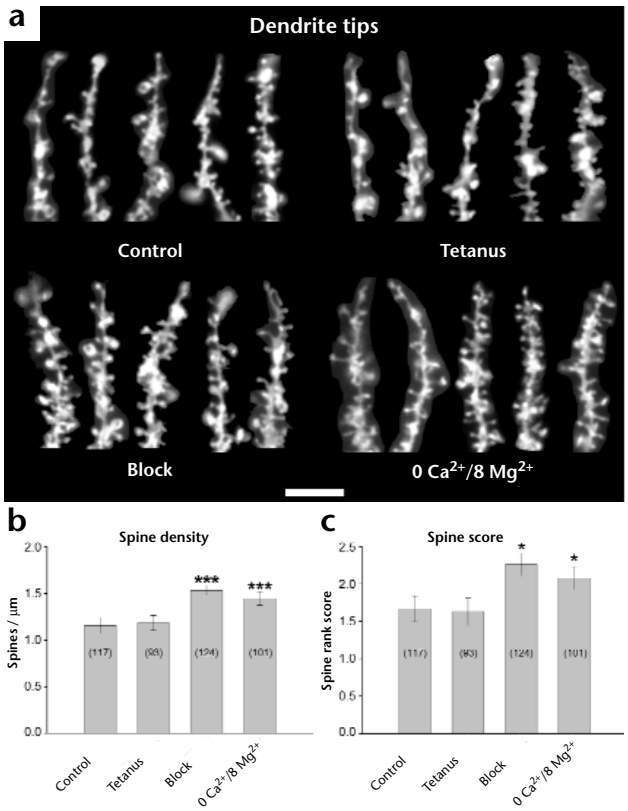

Fig. 3. Dendrite tips were spinier in slices with blocked synaptic transmission than in those under control or tetanus slice conditions. (**a**) Sets of high-magnification single-focal-plane images of the tips of five dendritic segments obtained in slices maintained in control or one of three experimental conditions. From left to right within each condition, spine density for these dendritic segments increases from the fiftieth to the ninetieth percentile in increments of ten. Scale bar, 5 µm. (**b**) Dendritic tips with higher spine densities occur more frequently in the block and 0 Ca^{2+}/8 Mg^{2+} conditions than in the control and tetanus conditions. (**c**) Spine rank scores were also higher in the block and 0 Ca^{2+}/8 Mg^{2+} conditions. Numbers of dendritic segments in each condition are indicated in parentheses within each bar. A total of 435 dendritic tips in 24 slices from six animals, that is six slices per experimental condition, are included. Asterisks indicate significant differences from the control and tetanized slice conditions (*$p < 0.05$; ***$p < 0.001$). Data are presented as mean ± s.e.

selective blocking of different components of synaptic and neuronal responses also affected spine density. Slices were maintained in control media with 2.5 mM Ca^{2+} and 1.3 mM Mg^{2+}, control media with APV and CNQX, control media with TTX or in a reduced-block, nominally calcium-free media with 8 mM Mg^{2+}, APV and CNQX (**Fig. 5**). The same procedures for imaging and analyzing the dendrites were used as described above, with all photography and analyses done blind with regard to experimental conditions.

Dendrites were more spiny in slices maintained in APV and CNQX, in TTX or in reduced block conditions as compared with the control condition ($F_{3,815} = 15.55$, $p < 0.001$; **Fig. 5a**). Spine density increased 10.4 ± 5.0% with TTX ($p < 0.005$, $n = 6$), 14.5 ± 4.9% with APV/CNQX ($p < 0.05$, $n = 4$) and 14.0 ± 3.1% under reduced block ($p < 0.001$, $n = 4$). Similarly, dendrites from the three block conditions had significantly higher spine rank scores than dendrites from control slices (**Fig. 5b**; χ^2 and ANOVA on ranks, $p < 0.001$). There were no significant differences in spine densities or scores among the slices treated with APV/CNQX, TTX or reduced block.

Electron microscopy was used to assess whether structurally healthy dendrites and synapses occurred under the different conditions of synapse inactivation. Healthy dendrites had intact membranes, uniformly spaced microtubules, clear cytoplasm and intact subcellular organelles. Well-preserved synapses had postsynaptic dendritic spines with a thickened postsynaptic density and presynaptic axonal varicosities with evenly distributed synaptic vesicles[26,29]. The dendrites and synapses were structurally intact in all conditions (**Fig. 6**).

Discussion

These findings show that new spines formed when synapses on mature hippocampal neurons were inactivated. The upward adjustment in spine number occurred at multiple locations, and not just at the tips, where new dendrites might have been added.

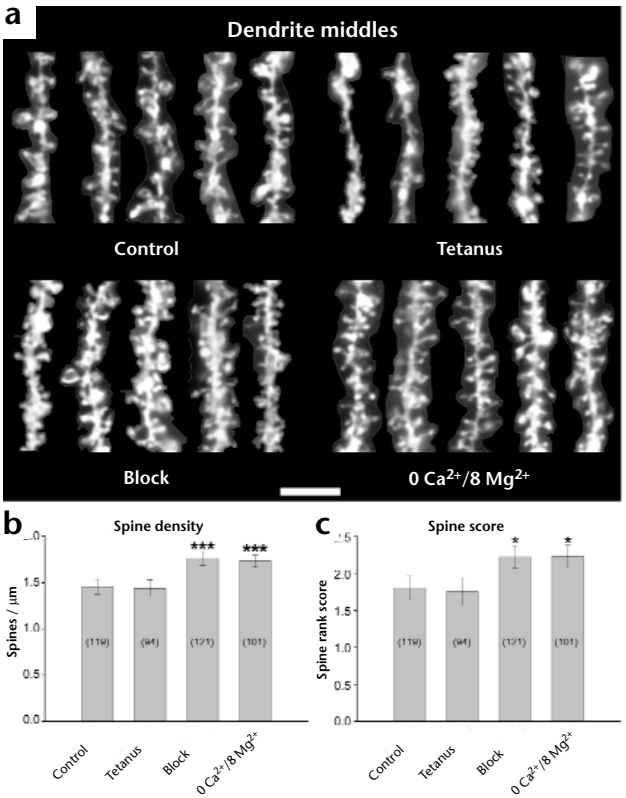

Fig. 4. Dendrite middles are spinier in slices with blocked synaptic transmission than in control or tetanus slice conditions. (**a**) High-magnification single-focal-plane images of the middle dendritic segments obtained in slices from control or experimental conditions indicated at the bottom of each condition. Spine density of dendritic segments within each condition increases from the fortieth (left) to the eightieth percentile (right) in increments of ten for each condition. Scale bar, 5 µm. (**b**) Spine densities and (**c**) spine rank scores across different slice conditions. The total number of dendritic segments in each condition is indicated within the parentheses in each bar, where 435 dendrite middles from 24 slices from six animals (six slices per experimental condition), are included. Asterisks indicate significant differences from the control and tetanus slice conditions (*$p < 0.05$; ***$p < 0.001$). Data are presented as mean ± s.e.

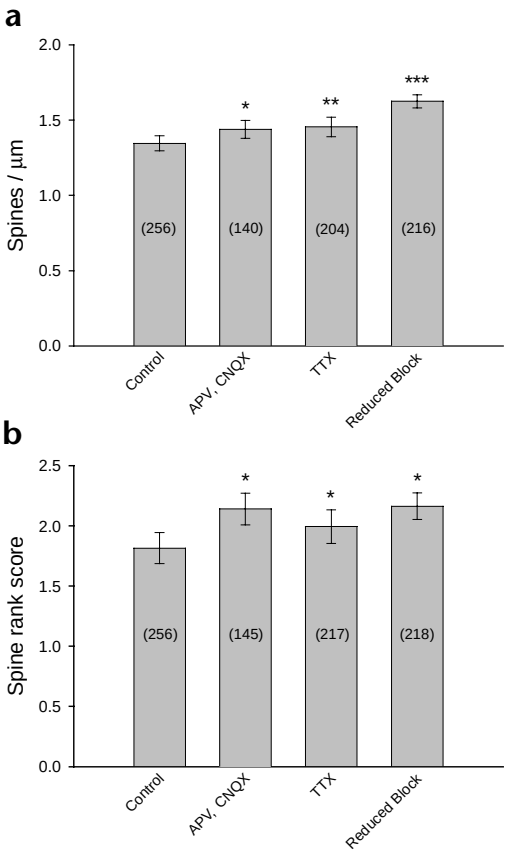

Fig. 5. Dendrites are also spinier with the selective block of presynaptic or postsynaptic activity. (**a**) Spine densities and (**b**) rank scores across different slice conditions. Data are from combined measures of dendrite tips and middles (mean ± s.e.) and the total number of dendritic segments are indicated within parentheses in each bar. Asterisks indicate significant increases from the control (*$p < 0.05$; **$p < 0.005$; ***$p < 0.001$).

It has long been postulated that spine number should increase to meet the demand of enhanced activity[32]. However, no consistent increase in spine or synapse number is detected on mature neurons with enhanced synaptic activation, such as long-term potentiation (LTP)[29,33,34]. Instead, mature neurons upregulate spine and synapse number when there is insufficient synaptic input, perhaps compensating for the lost input. It remains to be determined if all of the new spines have synapses under conditions of blocked synaptic activity, or if their number might decrease with the reinstatement of optimal activity.

Fewer spines occur in the hippocampus *in vivo* than in slices[26]. Thus, blocking synaptic activity does not merely preserve existing spines by protecting them from excitotoxicity in the slices[35], but leads to the induction of more spines. Ultrastructural observations showed that many intact synapses occurred under all of the different block conditions used here. Relative to neurons *in vivo*, neurons in control slices have more short and stubby, or mushroom-shaped, spines, which form synapses with pre-existing axonal boutons[26]. In addition to spines, long filopodia-like structures[4] occur in blocked slices.

The mechanisms by which reduced synaptic activity induces dendritic spines are unknown. All our experimental treatments that reduced activity also reduced postsynaptic calcium. In three of the block conditions, the extracellular calcium was nominally zero. The effect of the remaining extracellular calcium was minimized by high extracellular magnesium, ionotropic and metabotropic glutamate receptor antagonists, and/or nimodipine, the L-type calcium-channel blocker. The high extracellular magnesium would have stabilized the fixed negative charges of the plasma membrane[36], thereby preventing any epileptiform activity[37,38]. In other block conditions, where extracellular calcium was normal (2.5 mM), the calcium-permeable NMDA receptor was blocked by APV, and/or voltage-dependant influx of calcium was reduced with CNQX and TTX. Such a reduction in postsynaptic calcium permits enhanced actin polymerization[39,40], thereby supporting outgrowth of spine-like protrusions. Further study is required to determine if this permissive low-calcium environment is sufficient to trigger spine formation, or if other signaling cascades are responsible.

How long does it take for new spines to form on adult neurons? In dissociated cell culture, dendritic spines are highly motile structures, changing shape over minutes depending on the state of actin polymerization[41]. In organotypic slice cultures, dendritic protrusions appear and disappear in minutes[27], apparently in relationship to local activity[12]. Local potentiation of immature synapses in organotypic slice cultures leads to an outgrowth of spine-like protrusions 30 minutes later[13]. These observations suggest that new spines or filopodia can form quite rapidly on immature neurons. More spines occurred in mature slices within a couple of hours of making the slices[26], though shorter times have not yet been investigated.

How long can new spines last before they must be incorporated into a functional synaptic network? This is an intriguing question, because both anatomical and physiological evidence suggest that young, developing synapses have only NMDA glutamatergic receptors[42–45] and thus should be functionally silent.

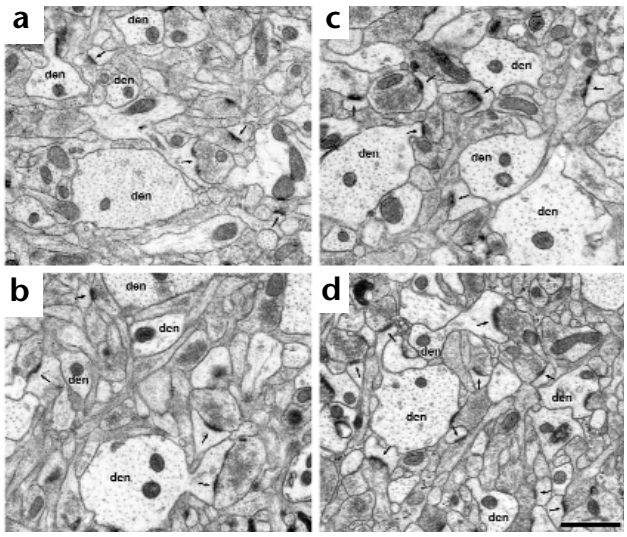

Fig. 6. Electron micrographs from neuropil in area CA1 of adult hippocampal slices. Morphologically healthy dendrites, spines, axons and synapses occur in (**a**) control (**b**) 0 Ca^{2+}/8 Mg^{2+} (**c**) block and (**d**) TTX slice conditions. Examples of well-preserved dendrites (den) and spines with synapses (→) are indicated. Scale bar, 1 µm.

Spine number remained elevated during eight hours of blocked synaptic activity, suggesting that new dendritic spines on mature hippocampal dendrites can persist for many hours in the absence of functional activity.

No global change in spine number was detected when synapses were activated with low-frequency control stimulation or repeated tetanic stimulation. In contrast, dendritic spines are lost after excessive activation, such as that which occurs after epileptic seizure[46–49]. Similarly, spines shorten[50] or immediately disappear[8] when cultured hippocampal neurons are exposed for only a few minutes to high concentrations of NMDA, which presumably causes excessive activity.

These findings suggest that mature neurons regulate total spine number according to the level of activity. Thus, spines and their synapses may be rapidly removed from an overly active network when the neuron is at risk of excitotoxicity. Conversely, inactive dendritic spines may persist for many hours, possibly providing a structural basis for the subsequent formation of functional synaptic networks.

Methods

Preparation and maintenance of hippocampal slices *in vitro*. Our procedures follow National Institutes of Health guidelines and undergo yearly review by the Animal Care and Use Committee at Children's Hospital. Mature male rats of the Long Evans strain, aged 60–82 days, were deeply anesthetized (at ~11:30 A.M., 4.5 h into their light cycle) with metofane (methoxyflurane) and decapitated. The right hippocampus was dissected from the rest of the brain and mounted on an agar block in a slicing chamber with partially frozen, oxygenated saline containing 234 mM sucrose, 5.3 mM KCl, 26 mM $NaHCO_3$, 1 mM NaH_2PO_4, 8 mM $MgSO_4$ and 10 mM glucose, pH 7.4. Transverse slices (400 μm) were cut from the middle third of the hippocampus with a vibrating-blade microtome (VT1000 S, Leica Instruments GmbH, Nussloch, Germany).

Two sets of experiments were performed, with six animals in each set. In the first set, slices were placed into each of three different ice-cold solutions equilibrated with 95% O_2/5% CO_2 at pH 7.4. The normal control medium contained 117 mM NaCl, 5.3 mM KCl, 26 mM $NaHCO_3$, 1 mM NaH_2PO_4, 2.5 mM $CaCl_2$, 1.3 mM $MgSO_4$ and 10 mM glucose. The nominally calcium-free medium contained this same solution except that it had 0 mM Ca^{2+} and 8 mM Mg^{2+}. The block medium also had 0 mM Ca^{2+} and 8 mM Mg^{2+}, as well as the activity antagonists tetrodotoxin (TTX, 1 μM), 6-cyano-7-nitroquinoxaline-2,3-dione (CNQX, 20 μM), D,L-2-amino-5-phosphonovaleric acid (APV, 50 μM), nimodipine (5 μM) and (S)-α-methyl-4-carboxyphenylglycine (MCPG, 500 μM). In the second set of experiments, slices were placed into one of the four ice-cold solutions equilibrated with a 95% O_2/5%CO_2 at pH 7.4. In addition to the normal control media, two solutions also contained ionotropic glutamate receptor antagonists CNQX (20 μM) and APV (50 μM) or the sodium channel blocker TTX (1 μM). The reduced block condition had 0 Ca^{2+} and 8 mM Mg^{2+}, CNQX (20 μM) and APV (50 μM).

Slices were transferred immediately into the recording chamber (Stoelting, Wood Dale, Illinois), placed onto nets positioned over one of four wells containing one of the media conditions, and maintained at the interface of humidified 95% O_2/5% CO_2 atmosphere at 32°C. The average delay between removal of the brain and placing the last slice into the recording chamber was about 15 minutes. CNQX and nimodipine were acquired from Research Biochemicals, (Natick, Massachusetts), TTX from Calbiochem (La Jolla, California), and MCPG from Tocris Cookson (Bristol, UK). All other drugs and chemicals were from Sigma Chemical (St. Louis, Missouri). MCPG was solubilized at 100× final concentration in 1.1 M NaOH. All other drugs were prepared at 1000× concentration in stock solutions.

DiI electrodes. Phenyl-substituted DiI (1,1′-dioctadecyl-5,5′-diphenyl-3,3,3′,3′-tetramethylindocarbocyanine chloride; Molecular Probes, Eugene, Oregon) was dissolved in *N,N*-dimethyformamide (0.5% weight per volume) and dried onto the tips of glass microelectrodes overnight at 60°C.

Physiological recordings. Slices were incubated in a recording chamber for about 3 hours. Two concentric bipolar stimulating electrodes (Ultrasmall, 25 μm pole separation; Fred Haer, Brunswick, Maine) were positioned 600–800 μm apart in the middle of stratum radiatum on either side of a single extracellular recording electrode (glass micropipet filled with 120 mM NaCl; **Fig. 1a**). Alternating stimuli (100 μs duration) were delivered at one per 15 s at an intensity that evoked field excitatory postsynaptic potentials (fEPSPs) with slopes of approximately 1 mV per ms. The fEPSPs were recorded with a microelectrode amplifier (Model 1800, A-M Systems, Carlsborg, Washington), filtered at 5 kHz, digitized at 29 kHz using an interface board (RC Electronics, Santa Barbara, California) and analyzed online with the Scope software (RC Electronics). The slope function (mV per ms) of the fEPSP was measured from the steepest 400 μs segment of the negative field potential.

Confocal microscopy. After a total of 8 h, slices were immersed in mixed aldehydes (0.1% glutaraldehyde, 4% paraformaldehyde in 0.1 M phosphate buffer) and brought to a final temperature of less than 37°C during 8 seconds of microwave irradiation[28]. Optimal preservation of CA1 pyramidal cells and their dendritic arbors occurred in the middle of the slices, as judged previously by EM[28,29] . The fixed slices were resectioned parallel to their surfaces at 100 μm with the Leica vibrating blade microtome. The two middle sections were mounted in buffer on glass slides, coverslipped, sealed with nail polish and coded. The dendrites were imaged by confocal scanning laser microscopy using the Noran OZ Confocal System (Noran, Middleton, Wisconsin) on a Nikon Diaphot 200 Inverted Microscope with a 100× oil objective (Nikon, n.a. 1.4). DiI fluorescence was excited by the 568 nm emission of a krypton-argon ion laser. Digital images were created by averaging 128 or 256 frames collected at a single focal plane at a resolution of 512 × 479 (8 bits per pixel). Each high magnification scan (1.5× electronic zoom) covered an area of 28.5 μm × 26.6 μm.

Image analysis. The imaging software entitled *IGL Trace* was used to compare images of the dendrites, and to position spine counts and measure dendritic lengths. This software is available at website: http://synapses.tch.harvard.edu/.

Several approaches for evaluating dendrite spininess were tested before settling on the two strategies used in this paper. In three of the experiments, we compared the spine density and rank scoring procedures with three-dimensional approaches by counting all spines occurring on each individual confocal section through a *z*-series of the dendrite, or counting all spines on a three-dimensional reconstruction made from the *z*-series (Intervision 3-D module, Noran). The percent increase in detectable spine density was less than 20% for the three-dimensional approaches, and the outcome of the experiments was identical for all four approaches. Thus, even with the three-dimensional approaches, the spine density of the mature neurons was too high to obtain accurate counts. We further attempted to overcome this problem by optically resectioning the dendrites perpendicularly; however, even with minimum separation, the *z* dimension was too great, and many spines either became disconnected from the parent dendrite or were still obscured by one another. In addition, it was much more time consuming to use any of the three-dimensional methods than to use spine density and rank scoring procedures.

Electron microscopy. Slices were fixed in mixed aldehydes containing 6% glutaraldehyde, 2% paraformaldehyde, 1 mM $CaCl_2$, and 2 mM $MgCl_2$, in 0.1 M cacodylate buffer at pH 7.4 during 8 s of microwave irradiation to ensure rapid fixation[28]. Tissue was processed for EM with osmium, uranyl acetate, dehydration and embedding in LX112 using standard microwave-enhanced procedures[4,26].

Statistical analysis. Control slices from different animals can have significantly different spine densities[29]. Hence, this potential bias was avoided by using within-animal scoring procedures. A two-way ANOVA, followed by Tukey's post-hoc method, was used to evaluate what part of the spine-density variance between dendrites arose from different experimental conditions and what part was due to differences between animals. The χ^2-test and Kruskal-Wallis ANOVA on ranks, followed by

Dunn's post-hoc test, were used for the spine rank scoring procedure. The significance criterion was set at $p < 0.05$.

Acknowledgements

We thank J. Fiala for improving IGL Trace for use with confocal microscopy and for his input on this work. We also thank M. Feinberg and A. Goddard for technical support. This work was supported by NIH grants NS21184, NS33574, MH/DA57351, which is funded jointly by NIMH, NIDA, NASA (K.M.H) and the Mental Retardation Research Center grant P30-HD18655 to Joseph Volpe.

RECEIVED 23 JUNE ; ACCEPTED 12 AUGUST 1999

1. Gray, E. G. Axo-somatic and axo-dendritic synapses of the cerebral cortex: An electron microscopic study. *J. Anat.* **93**, 420–433 (1959).
2. Harris, K. M. & Kater, S. B. Dendritic spines: Cellular specializations imparting both stability and flexibility to synaptic function. *Annu. Rev. Neurosci.* **17**, 341–371 (1994).
3. Harris, K. M., Jensen, F. E. & Tsao, B. Three-dimensional structure of dendritic spines and synapses in rat hippocampus (CA1) at postnatal day 15 and adult ages: Implications for the maturation of synaptic physiology and long-term potentiation. *J. Neurosci.* **12**, 2685–2705 (1992).
4. Fiala, J. C., Feinberg, M., Popov, V. & Harris, K. M. Synaptogenesis via dendritic filopodia in developing hippocampal area CA1. *J. Neurosci.* **18**, 8900–8911 (1998).
5. Papa, M., Bundman, M. C., Greenberger, V. & Segal, M. Morphological analysis of dendritic spine development in primary cultures of hippocampal neurons. *J. Neurosci.* **15**, 1–11 (1995).
6. Papa, M. & Segal, M. Morphological plasticity in dendritic spines of cultured hippocampal neurons. *Neuroscience* **71**, 1005–1011 (1996).
7. Kossel, A. H., Williams, C. V., Schweizer, M. & Kater, S. B. Afferent innervation influences the development of dendritic branches and spines via both activity-dependent and non-activity-dependent mechanisms. *J. Neurosci.* **17**, 6314–6324 (1997).
8. Halpain, S., Hipolito, A. & Saffer, L. Regulation of F-actin stability in dendritic spines by glutamate receptors and calcineurin. *J. Neurosci.* **18**, 9835–9844 (1998).
9. Annis, C. M., O'Dowd, D. K. & Robertson, R. T. Activity-dependent regulation of dendritic spine density on cortical pyramidal neurons in organotypic slice cultures. *J. Neurobiol.* **25**, 1483–1493 (1994).
10. McAllister, A. K., Katz, L. C. & Lo, D. C. Neurotrophin regulation of cortical dendritic growth requires activity. *Neuron* **17**, 1057–1064 (1996).
11. Collin, C., Miyaguchi, K. & Segal, M. Dendritic spine density and LTP induction in cultured hippocampal slices. *J. Neurophysiol.* **77**, 1614–1623 (1997).
12. Maletic-Savatic, M., Malinow, R. & Svoboda, K. Rapid dendritic morphogenesis in CA1 hippocampal dendrites induced by synaptic activity. *Science* **283**, 1923–1927 (1999).
13. Engert, F. & Bonhoeffer, T. Dendritic spine changes associated with hippocampal long-term synaptic plasticity. *Nature* **399**, 66–70 (1999).
14. Dalva, M. B., Ghosh, A. & Shatz, C. J. Independent control of dendritic and axonal form in the developing lateral geniculate nucleus. *J. Neurosci.* **14**, 3588–3602 (1994).
15. Rocha, M. & Sur, M. Rapid acquisition of dendritic spines by visual thalamic neurons after blockade of N-methyl-D-aspartate receptors. *Proc. Natl. Acad. Sci. USA* **92**, 8026–8030 (1995).
16. Bravin, M., Morando, L., Vercelli, A., Rossi, F. & Strata, P. Control of spine formation by electrical activity in the adult rat cerebellum. *Proc. Natl. Acad. Sci. USA* **96**, 1704–1709 (1999).
17. Turrigiano, G. G., Leslie, K. R., Desai, N. S., Rutherford, L. C. & Nelson, S. B. Activity-dependent scaling of quantal amplitude in neocortical neurons. *Nature* **391**, 892–896 (1998).
18. Woolley, C. S., Gould, E., Frankfurt, M. & McEwen, B. S. Naturally occurring fluctuation in dendritic spine density on adult hippocampal pyramidal neurons. *J. Neurosci.* **10**, 4035–4039 (1990).
19. Gould, E., Woolley, C. S., Frankfurt, M. & McEwen, B. S. Gonadal steroids regulate dendritic spine density in hippocampal pyramidal cells in adulthood. *J. Neurosci.* **10**, 1286–1291 (1990).
20. Greenough, W. T. & Bailey, C. H. The anatomy of a memory: Convergence of results across a diversity of tests. *Trends Neurosci.* **11**, 142–147 (1988).
21. Bailey, C. H. & Kandel, E. R. Structural changes accompanying memory storage. *Annu. Rev. Physiol.* **55**, 397–426 (1993).
22. Moser, M. B., Trommald, M. & Andersen, P. An increase in dendritic spine density on hippocampal CA1 pyramidal cells following spatial learning in adult rats suggests the formation of new synapses. *Proc. Natl. Acad. Sci. USA* **91**, 12673–12675 (1994).
23. Boyer, C., Schikorski, T. & Stevens, C. F. Comparison of hippocampal dendritic spines in culture and in brain. *J. Neurosci.* **18**, 5294–5300 (1998).
24. McKinney, R. A., Capogna, M., Durr, R., Gahwiler, B. H. & Thompson, S. M. Miniature synaptic events maintain dendritic spines via AMPA receptor activation. *Nat. Neurosci.* **2**, 44–49 (1999).
25. Harris, K. M. Structure, development, and plasticity of dendritic spines. *Curr. Opin. Neurobiol.* **9**, 343–348 (1999).
26. Kirov, S. A., Sorra, K. E. & Harris, K. M. Slices have more synapses than perfusion-fixed hippocampus from both young and mature rats. *J. Neurosci.* **19**, 2876–2886 (1999).
27. Dailey, M. E. & Smith, S. J. The dynamics of dendritic structure in developing hippocampal slices. *J. Neurosci.* **16**, 2983–2994 (1996).
28. Jensen, F. E. & Harris, K. M. Preservation of neuronal ultrastructure in hippocampal slices using rapid microwave-enhanced fixation. *J. Neurosci. Methods* **29**, 217–230 (1989).
29. Sorra, K. E. & Harris, K. M. Stability in synapse number and size at 2 hr after long-term potentiation in hippocampal area CA1. *J. Neurosci.* **18**, 658–671 (1998).
30. Trommald, M., Jensen, V. & Andersen, P. Analysis of dendritic spines in rat CA1 pyramidal cells intracellularly filled with a fluorescent dye. *J. Comp. Neurol.* **353**, 260–274 (1995).
31. Rusakov, D. A. & Stewart, M. G. Quantification of dendritic spine populations using image analysis and a tilting disector. *J. Neurosci. Methods* **60**, 11–21 (1995).
32. Horner, C. H. Plasticity of the dendritic spine. *Prog. Neurobiol.* **41**, 281–321 (1993).
33. Chang, F. L. & Greenough, W. T. Lateralized effects of monocular training on dendritic branching in adult split-brain rats. *Brain Res.* **232**, 283–292 (1982).
34. Andersen, P. & Soleng, A. F. Long-term potentiation and spatial training are both associated with the generation of new excitatory synapses. *Brain Res. Brain Res. Rev.* **26**, 353–359 (1998).
35. Choi, D. W. Glutamate neurotoxicity and diseases of the nervous system. *Neuron* **1**, 623–634 (1988).
36. Frankenhaeuser, B. & Hodgkin, A. L. The action of calcium on the electrical properties of squid axons. *J. Physiol. (Lond.)* **137**, 218–244 (1957).
37. Taylor, C. P. & Dudek, F. E. Synchronous neural afterdischarges in rat hippocampal slices without active chemical synapses. *Science* **218**, 810–812 (1982).
38. Haas, H. L. & Jefferys, J. G. Low-calcium field burst discharges of CA1 pyramidal neurones in rat hippocampal slices. *J. Physiol. (Lond.)* **354**, 185–201 (1984).
39. Fifkova, E. Actin in the nervous-system. *Brain Res.* **9**, 187–215 (1985).
40. Janmey, P. A. Phosphoinositides and calcium as regulators of cellular actin assembly and disassembly. *Annu. Rev. Physiol.* **56**, 169–191 (1994).
41. Fischer, M., Kaech, S., Knutti, D. & Matus, A. Rapid actin-based plasticity in dendritic spines. *Neuron* **20**, 847–854 (1998).
42. Nusser, Z. *et al.* Cell type and pathway dependence of synaptic AMPA receptor number and variability in the hippocampus. *Neuron* **21**, 545–559 (1998).
43. Gomperts, S. N., Rao, A., Craig, A. M., Malenka, R. C. & Nicoll, R. A. Postsynaptically silent synapses in single neuron cultures. *Neuron* **21**, 1443–1451 (1998).
44. Petralia, R. S. *et al.* Selective acquisition of AMPA receptors over postnatal development suggests a molecular basis for silent synapses. *Nat. Neurosci.* **2**, 31–36 (1999).
45. Shi, S. H. *et al.* Rapid spine delivery and redistribution of AMPA receptors after synaptic NMDA receptor activation. *Science* **284**, 1811–1816 (1999).
46. Paul, L. A. & Scheibel, A. B. Structural substrates of epilepsy. *Adv. Neurol.* **44**, 775–786 (1986).
47. Jiang, M., Lee, C. L., Smith, K. L. & Swann, J. W. Spine loss and other persistent alterations of hippocampal pyramidal cell dendrites in a model of early-onset epilepsy. *J. Neurosci.* **18**, 8356–8368 (1998).
48. Muller, M., Gahwiler, B. H., Rietschin, L. & Thompson, S. M. Reversible loss of dendritic spines and altered excitability after chronic epilepsy in hippocampal slice cultures. *Proc. Natl. Acad. Sci. USA* **90**, 257–261 (1993).
49. Drakew, A., Muller, M., Gahwiler, B. H., Thompson, S. M. & Frotscher, M. Spine loss in experimental epilepsy: quantitative light and electron microscopic analysis of intracellularly stained CA3 pyramidal cells in hippocampal slice cultures. *Neuroscience.* **70**, 31–45 (1996).
50. Segal, M. Morphological alterations in dendritic spines of rat hippocampal neurons exposed to N-methyl-D-aspartate. *Neurosci. Lett* **193**, 73–76 (1995).